Geothermal Gradients and Geothermal Opportunities in the Piceance Basin, Colorado

Paul Morgan, Colorado Geological Survey, 1313 Sherman Street, Room 715, Denver, CO 80203: morgan@mines.edu

1. Abstract

Bottom-hole temperature (BHT) data have been compiled from 10,372 hydrocarbon wells in the Piceance basin with an average depth of 2103 ± 685 (± standard deviation) m. For a preliminary statistical analysis, the data were combined in 0.4 by 0.4 degree blocks by their geographic coordinates and average geothermal gradients calculated for each block. Gradients ranged from 22.7 to 41.8°C/km. Block gradients corrected for the disturbance caused by drilling ranged from 27.3 to 51.5°C.km. Uncorrected BHTs indicate geothermal resources at temperatures of 100 to 250°C at depths of 2.5 to 5 km. Corrected BHTs reduce these depths to 1.7 to 4.2 km. Generally permeability at these depths is low. The Leadville Limestone, a Mississippian karst-forming limestone is likely to underlie most of the basin, shallowing on the southwest margin of the basin. Observations of this limestone at other locations indicate that it is a very permeable aquifer. Production from similar fractured karst limestone aquifers in Germany has generated ≥3.0 MWe from single wells. Alternatively, impermeable strata could be hydrofractured to produce an enhanced/engineered geothermal system (EGS). In addition to power production, geothermal systems are being investigated in northern Alberta, Canada, as a source of thermal energy for *in situ* extraction of hydrocarbons from oil sands. The Piceance Basin is one of the largest know reservoirs of oil shale in the world and geothermal energy could be used to preheat the oil shale prior to extraction of hydrocarbons from this resource. Geothermal energy is an environmentally clean source of energy for these processes. There is very little produced water with hydrocarbon extraction in the Piceance Basin and geothermal energy from co-produced fluids in the basin is unlikely.

2. Introduction and Reduction of Data

The physiographic Piceance Basin is shown in Figure 1 and comprises four drainage basins, the Yellow Creek, the Piceance Creek, the Roan Creek, and the Parachute Creek Drainage Basins. The structural basin is significantly larger in area, as shown by a map of the generalized depth to the base of coal in Upper Cretaceous Cameo Group, shown in Figure 2. It is generally designated as a Laramide-age basin but it occupies part of the Early Pennsylvanian Maroon Trough (Quigley, 1965). Before the Maroon Trough, the area was a marine seaway. Mississippian shelf and platform limestone and dolomite of this seaway in northwestern Colorado range from zero to 210 m in thickness. These rocks are the local representative of the Leadville Limestone which has equivalents in the Four Corner states and Wyoming and are

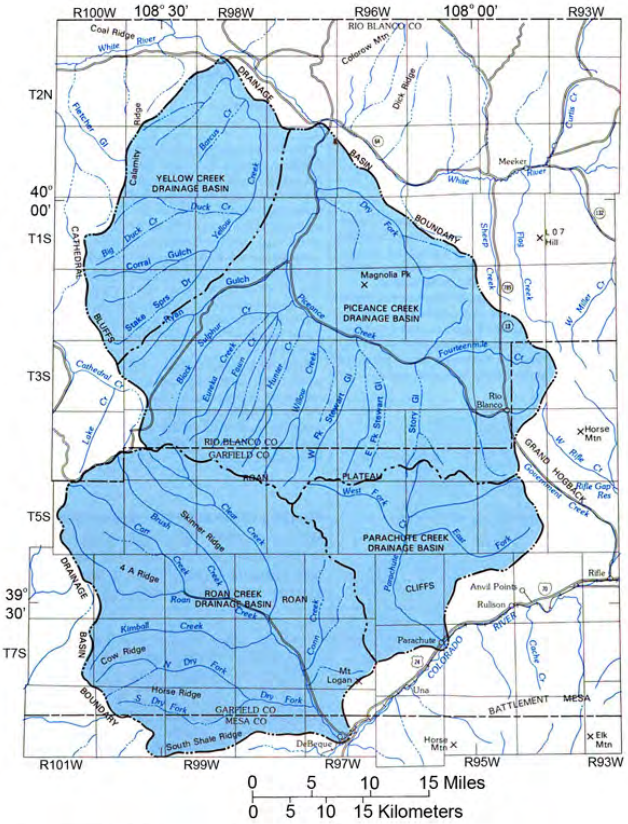

Figure 1. Piceance Drainage basin showing component drainage basins. Modified from Taylor (1987, Figure 3)

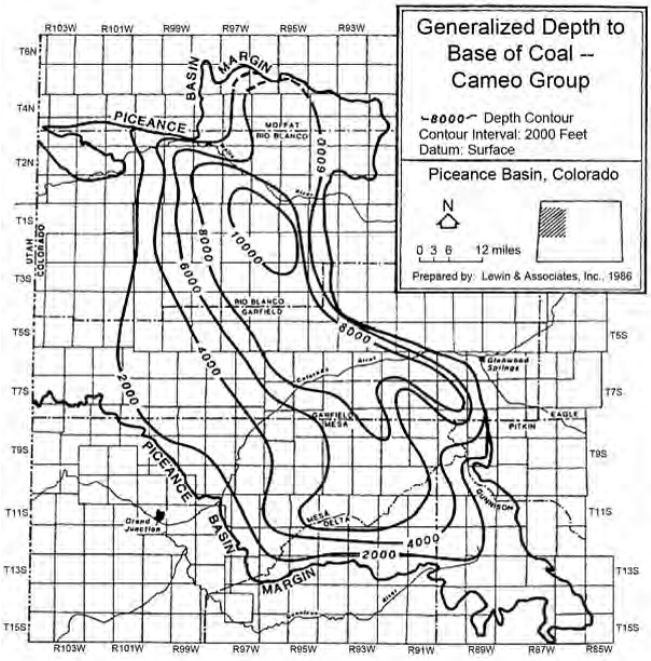

Figure 2. Piceance Basin - generalized depth to base of Cameo Group coal. Modified from EPA (2004, Attachment 3, Figure A3-3).

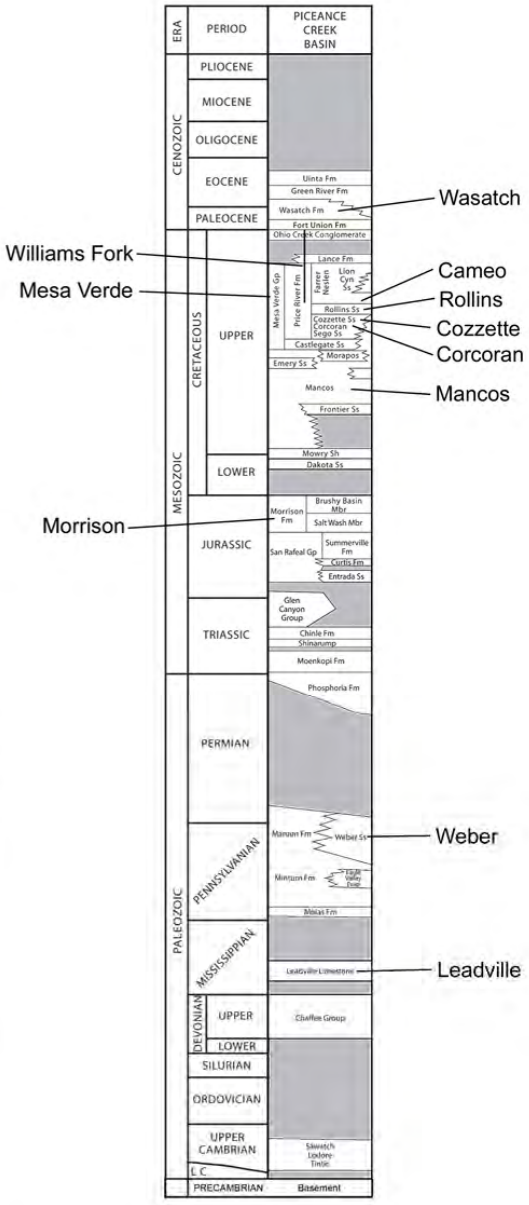

Figure 3. Generalized Stratigraphic Column for the Piceance Basin. Modified from CGS (unpublished)

typically karst-forming limestones. Continued growth of the Ancestral Front Range and Uncompahgre Uplift continued to act as sources for clastics, carbonates, and evaporites in the trough from Late Permian through the Jurassic. A marine transgression in the Cretaceous resulted in renewed sedimentation and the basin became a shallow sea with lagoonal and swamp sediments. At the end of the Cretaceous the basin was folded and faulted during the Laramide orogeny forming the present tectonic Piceance Basin (Quigley, *op. cit*.). A generalized stratigraphic column for the Piceance basin is shown in Figure 3.

The complete BHT data set compiled from 10,372 oil and gas wells is plotted as a function of depth in Figure 4. Table 1 lists average geothermal gradients from the surface for wells terminating in different units: the only unit that has a gradient that is statistically significant is the Lower Permian/Upper Pennsylvanian Weber unit. This unit has a greater thickness of Upper Paleozoic sedimentary rocks than all other units in the table. These rocks have a higher proportion of high thermal conductivity limestone, dolomite and evaporates and shallower formations and the drop in thermal gradient is probably associated with a change in thermal conductivity. These data are not corrected for the transient temperature disturbance caused by the circulation of drilling fluid. Temperature data from drill-stem tests (DST data) are often taken to be a close approximation to the undisturbed, or virgin rock temperatures (VRTs). DSTs pull fluid from a formation under test which is generally assumed to be outside the region of thermal (and fluid) disturbance by drilling. In some wells, a second cement-bond log (CBL) is run days, weeks, or months (rare) after normal logging operations and a BHT may be measured on this log. These second cement bond log temperatures may also be a close approximations to the VRTs. In this study, data from DSTs and CBLs will be referred to as *proxy VRTs*.

Table 1. Depth, BHT and geothermal gradient data for different units.

Stratigraphic Age	Name	Average Depth, m	Average Temperature, °C	Geothermal Gradient, °C/km	n
Paleocene/Eocene	WASATCH	917 ± 471	44 ± 15	39 ± 15	181
Upper Cretaceous	WILLIAMS FORK	2183 ± 549	89 ± 24	36 ± 12	664
Upper Cretaceous	MESA VERDE	1756 ± 772	65 ± 25	33 ± 11	238
Upper Cretaceous	CAMEO	2320 ± 432	93 ± 19	35 ± 6	477
Upper Cretaceous	ROLLINS	2367 ± 401	99 ± 19	37 ± 6	4605
Upper Cretaceous	COZZETTE	2139 ± 568	89 ± 23	38 ± 7	68
Upper Cretaceous	CORCORAN	2287 ± 745	88 ± 24	35 ± 6	956
Upper Cretaceous	MANCOS	1353 ± 589	55 ± 25	34 ± 8	563
Upper Jurassic	MORRISON	1622 ± 642	63 ± 20	34 ± 7	255
Lower Permian/Upper Pennsylvanian	WEBER	1985 ± 213	64 ± 9	26 ± 3	464

For the Piceance Basin, limited DST and CBL temperature data are available, and these are plotted together with normal BHT data from the same wells in Figure 5. The wells sampled by the DST and CBL data sets overlap geographically but cover different areas. They have different average mean temperatures and average thermal gradients. Both data sets show that the BHTs are cooler than the *proxy VRTs* but do not indicate a common correction. When the averages from each data set are examined, however, there is remarkable agreement in the disturbances indicated by the two data sets. For each data set the average temperatures and depths were calculated and then the temperatures were corrected to 2000 m using the temperature gradients calculated from the linear fits to the data shown in Figure 5. The difference was then calculated between the *proxy VRTs* at 2000 m and the normal BHT temperatures at 2000 m. For both the CBL and the DST data sets this difference was calculated to be 8.7°C. This agreement is perhaps fortuitous, but the magnitude of the correction is consistent with the BHT corrections for other basins (*e.g.*, Harrison *et al.*, 1983, Blackwell and Richards, 2004). A BHT correction has therefore been calculated from the average of the differences of the pairs of the CBL and DST lines, and this correction is:

$$T_{corr} = 0.00175z + 5.0685 \text{ °C} \quad (1)$$

where T_{corr} is the correction in °C, and z is depth in meters. As a rough check on this crude estimate of the correction, the calculated correction at 2000 m is 8.6°C. All values calculated using this correction are indicated as "corrected" values below. Corrected BHTs are plotted as a function of depth in Figure 6.

Roan Cliffs, exposing hundreds of feet of Green River Formation. Photo Credit: Vince Matthews, CGS

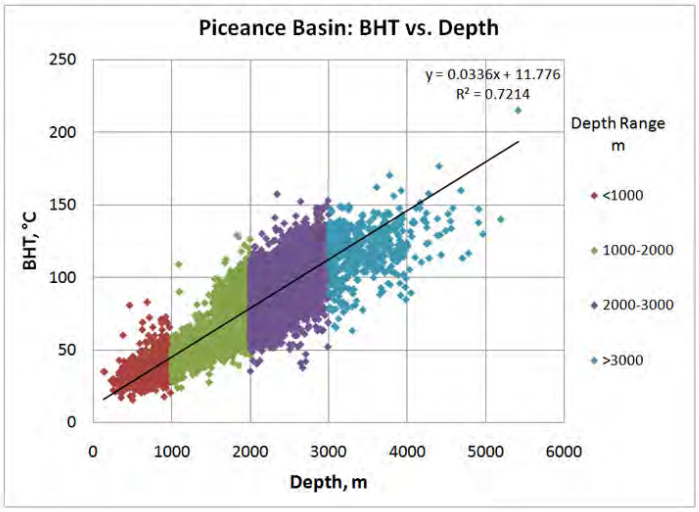

Figure 4. Uncorrected Bottom-Hole-Temperature (BHT) data from the Piceance Basin plotted as a function of loggers depth

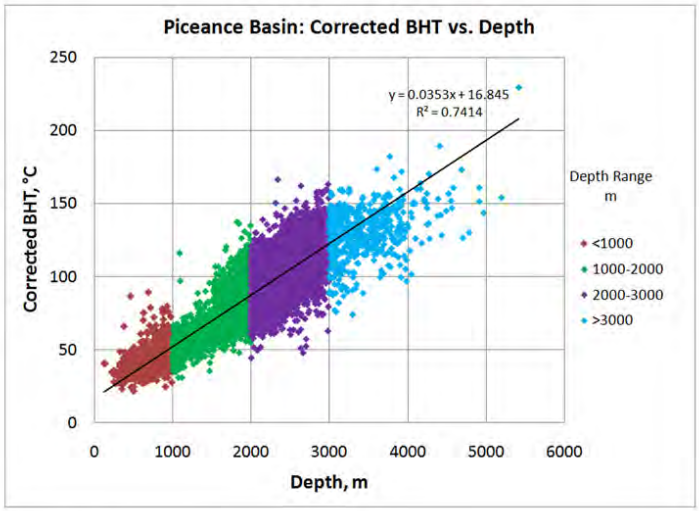

Figure 5. Corrected BHT data from the Piceance Basin plotted as a function of loggers depth

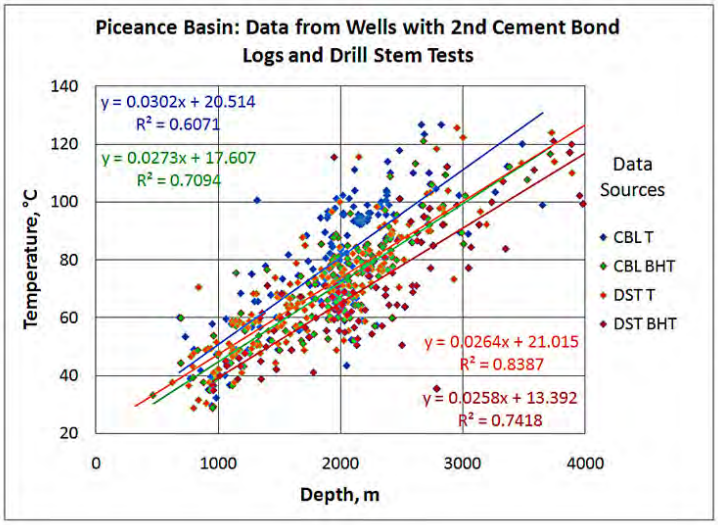

Figure 6. Temperature data vs. depth for wells with DSTs and CBLs (see text for details). CBLTs are BHT data from 2nd cement bond logs; CBL BHTs are uncorrected BHT data from wells with 2ndcement bond logs. DST Ts are temperature data from drill stem tests; DST BHT are uncorrected BHT data from wells drill stem tests. Linear trendline fits and parameters of fit are given for each dataset with colors matching dataset

3. Calculation of Geothermal Gradients

For calculation of temperature gradients, an estimate of the surface ground temperature is required. For this study surface air temperature data were compiled from the Western Regional Climate Center (URL: wrcc@dri.edu, last accessed 2011-5-11). Temperature data were collected from twenty one climate stations in and around the Piceance Basin and a linear fit was made to the temperature versus elevation data from these stations with the following result:

$$T_{sa} = 20.085 - 0.007027e \text{ °C} \quad (2)$$

where T_{sa} is the surface air temperature in °C and e is elevation in m. The goodness of fit parameter (R^2) for this fit was 0.8. The data were also analyzed in terms of a dependence on latitude and/or longitude, but no significant correlation with these parameters was found. Previous studies have found that, on average, surface ground temperature are 3°C higher than surface air temperature, and therefore the following formula was used to calculate surface temperatures for each well:

$$T_s = 23.085 - 0.007027e \text{ °C} \quad (3)$$

where T_s is the surface ground temperature in °C.

Geothermal gradients were estimated by two methods. The first method used trendline fits to plots of temperature vs. depth using Microsoft Excel®: gradients calculated by this method are given in Figures 5 and 6. The second method calculated gradients for individual wells as:

$$\partial T/\partial z = (T - T_s)/z \quad (4)$$

where $\partial T/\partial z$ is the geothermal gradient and T is temperature at depth z: gradients calculated by this method are displayed in Figure 7. With z in km, the units for geothermal gradient are °C/km.

Geothermal gradients were averaged in 0.4 by 0.4 degree blocks and plotted at their average geographic coordinate location in Figure 7. The number of data in each block is indicated in parentheses by the symbol that indicates the average geothermal gradient in each block. The outlines of the physiographic and structure Piceance Basins from Figures 1 and 2, respectively, are also shown on Figure 7. There is a clear trend of increasing gradients from north to south. Figure 8 is a plot of average well depths corresponding to Figure 7. Comparing Figures 7 and 8 suggests an imperfect inverse correlation between average geothermal gradient and average well depth. Lower geothermal gradients tend to be found where the basin is deeper, although a very well established uncorrected gradient of 39.2°C/km was calculated in the second most populated block (n = 2652) with an average depth of 2170 m. Uncorrected average block gradients ranged from 22.7 to 41.8°C/km; corrected average block gradients ranged from 27.3 to 51.5°C/km.

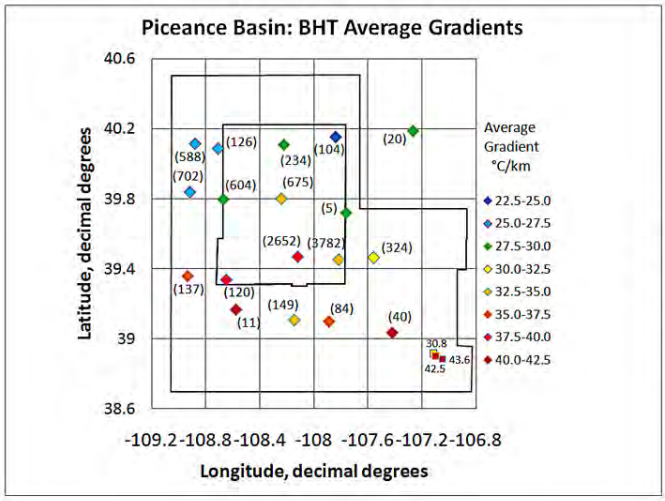

Figure 7. Average corrected BHT gradients calculated in 0.4 by 0.4 degree blocks and plotted at the average coordinates of the wells in the block. Number in parentheses is the number of wells in the block. Data in lower right block are gradient from individual heat-flow sites. Data points are color-coded by average gradient.

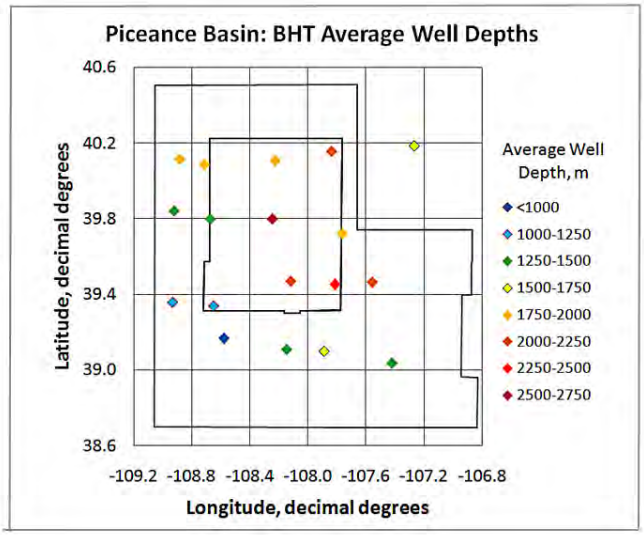

Figure 8. Average well depths for wells for wells in 0.4 by 0.4 degree blocks used for the average gradient calculations in Figure 7. Points are plotted at the average coordinate of the wells in each block. Data points are color-coded by depth.

Coal Canyon near Palisade with Williams Fork Formation on the north flank and Rollins Sandstone in the foreground
Photo credit: Ralph Topper, CGS

4. Interpretation of Results

There is a weak inverse correlation between average geothermal gradient and average well depth (R^2 = 0.11), as shown in Figure 9. The large scatter in this plot strongly suggests that geothermal gradient is not controlled by changes in mean thermal conductivity associated with lithologic changes, for which well depth is a proxy. Assuming that the main production horizons are similar across the basin, average well depth is a function of the depths to the main production layers. If thinning of sedimentary rocks overlying the main production horizons as their depths change is partially by pinching out of some horizons, then the lithologic column above the main producing horizons would be expected to change. Changes in the lithologic column are likely to be accompanied by changes in the mean thermal conductivity of the column resulting in changes in geothermal gradient even for uniform heat flow. However, as there is no simple relation between average geothermal gradient and average well depth, factors other than changes in mean thermal conductivity with depth may be assumed to dominate.

Heat is redistributed by groundwater flow in many sedimentary basins (*e.g.*, the Raton Basin, Colorado; Morgan, 2009). An indication that groundwater thermal convection may be occurring is that there is a general inverse correlation among geothermal gradients calculated for individual wells and the collar elevations for the wells. A more accurate indicator is to plot the elevation of the water table at each well, but well collar elevation is a useful proxy for water table elevation if the number of wells is large. A plot of geothermal gradients versus collar elevation for individual wells is shown in Figure 10. For the Piceance Basin the correlation is

weak (R^2 = 0.16) but it is positive rather than negative. The plot of geothermal gradient versus well collar elevation does not indicate large-scale thermal convection driven by regional groundwater recharge.

The general increase in geothermal gradient from north to south in the Piceance basin cannot be explained by a general lithologic change associated with well depth or with groundwater convection. The Upper Cretaceous depocenter of the basin is to the north. The depocenter is relatively narrow to the north, and locally higher geothermal gradients are where this depocenter is relatively deep north of latitude 39.4°N (Figure 7). However, south of latitude 39.4°N the higher geothermal gradients do not spatially correlate with the depocenter. High geothermal gradients from equilibrium heat flow measurements are in the southeast corner of the study area at the extreme edge of the depocenter and indicate that the high gradients are a regional anomaly, not a result of thermal refraction associated with basin structure.

A conspicuous source of the regional, high geothermal gradients at the southern end of the Piceance basin is not obvious. However, other geological features commonly associated

with elevated heat flow are observed. A northwest trending system of late Tertiary and Quaternary faults follows the northeastern margin of the Uncompahgre Uplift on the southwest of the Basin, as shown in Figure 11. Basaltic lava flows are exposed approximately 40 km east-southeast of Grand Junction, also shown in Figure 11. The flows include Grand Mesa, a flat-topped mountain over 1,500 km^2 in area. The flows are approximately 10 Ma old. Individual flows range from about 60 to more than 180 m in thickness. Although basaltic lavas typically rise through the upper crust rapidly, transferring little heat, such a major series of flows indicates that there must have been a significant energy source in the upper mantle responsible for their generation. Heat dissipates from shallow igneous intrusions in a much shorter time interval than 10 Ma, but a heat source at lower crustal or upper mantle depths could still have an effect at the surface after 10 Ma. Thus the very young faulting and Miocene volcanism support the hypothesis of a deep origin for the elevated geothermal gradients in the southern Piceance basin. High gradients, modified as appropriate by thermal conductivity changes with lithology, may be expected to continue beneath the measured BHT depths.

Frozen waterfall of drilling fluid, Garden Gulch, Piceance Basin. Photo Credit: SkyTruth/ Foter.com / CC BY-NC-SA (Open education-use, non-commercial license: do not reproduce without permission of copyright owner)

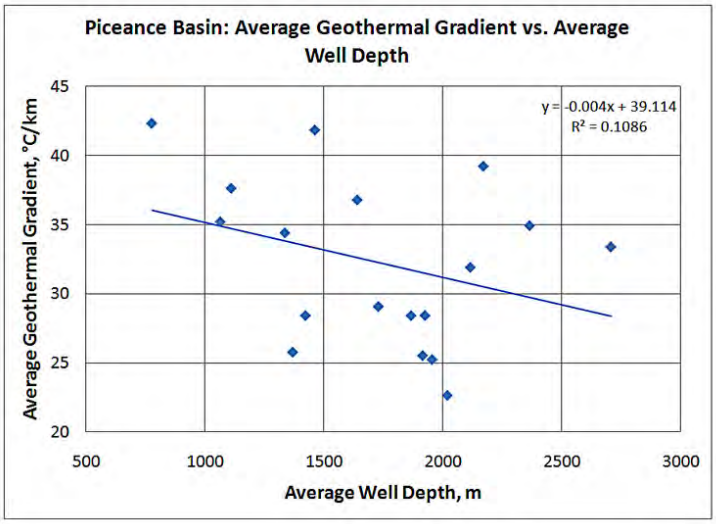

Figure 9. Average geothermal gradient (Fig. 7) vs. average well depth (Fig. 8)

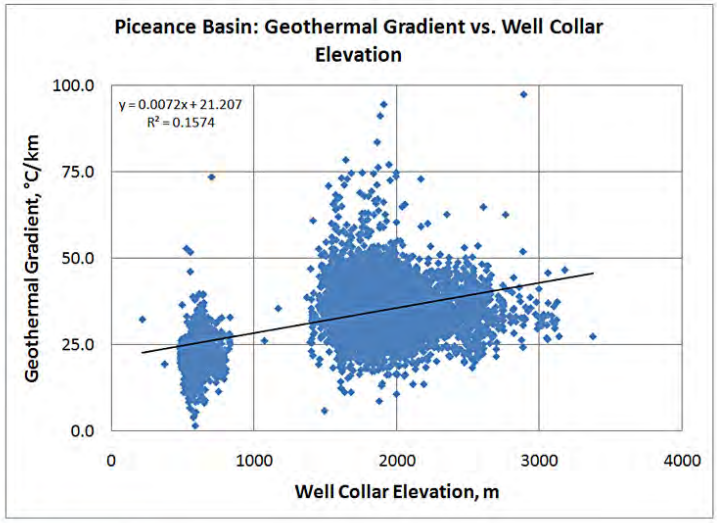

Figure 10. Geothermal gradients calculated from individual wells vs. the collar elevations of the wells.

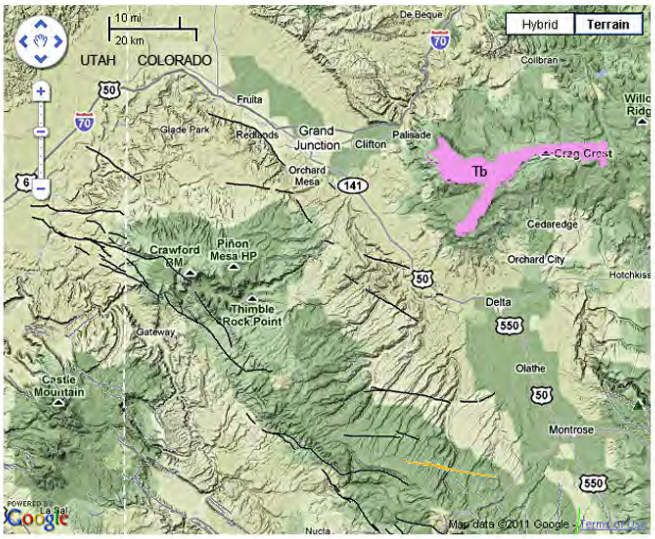

Figure 11. Topography, Quaternary faults, and remnants of lava flow at the southern end of the Piceance Basin. Tb indicates Tertiary (10 Ma) basalt flow. Black lines are Quaternary faults. Modified from Google.

5. Geothermal Resources in the Piceance Basin

There are two options for producing high volumes of geothermal fluid from depth in the Piceance Basin, 1. find a naturally permeable aquifer or 2. stimulate permeability. Two ≥3 MWe geothermal power plants in Germany use natural permeability in a fractured limestone that has significant karst (cave) permeability. A shallow-water limestone was deposited across most of the Four Corner states and into Wyoming during the Mississippian period, and wherever this limestone is exposed today it is observed to have karst permeability. It has different names in different states: the Redwall Limestone in Arizona, the Redwall or Leadville Limestone in Utah, the Leadville Limestone in Colorado and northwestern New Mexico, and the Madison Limestone in Wyoming. Large caves are observed where the Redwall Limestone crops out as a steep cliff-forming formation in Arizona's Grand Canyon, but its cave-forming properties may be observed in the neighboring Colorado Plateau by depressions as the overlying strata have collapsed into voids in the buried Redwall to form sedimentary breccia pipes. From these indications of subsurface caves in the Redwall, we may assume that the Mississippian limestone is likely to have karst structure throughout the region. Regional structural contours on the top of the Mississippian by Casillas (2004, Figure 50), based on the modeling of gravity and seismic data, indicate that this surface shallows from a maximum depth of about 3,000 m below sea level in the Piceance Basin to about 300 m below sea level on the southwestern margin of the basin. The Leadville Limestone is seen to have major karst properties wherever it outcrops in the Piceance Basin, such as around Glenwood Springs (Figures 12 and 13).

Figure 12 (above). Outcrop of Leadville Limestone just south of I-70 on the east side of Glenwood Springs.

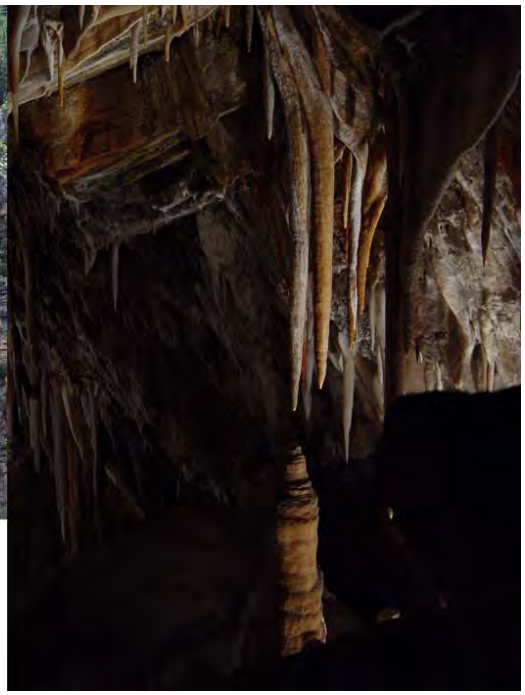

Figure 13 (right). Cavern in the Leadville Limestone on the north side of Glenwood Springs.

6. Geothermal from Co-Produced Water in the Piceance Basin

In common with most oil and gas production in Colorado (the exception is coalbed methane), there is very little co-produced water with oil and gas in the Piceance Basin. Figure 14 shows water production with first gas production and the changes over a five-year interval from a group of gas wells in the Wasatch Formation, Parachute Field in the Piceance Basin. For most of these wells there was no water production. In wells where there is water production it generally decreases with time, but there are exceptions (Nelson and Santus, 2010).

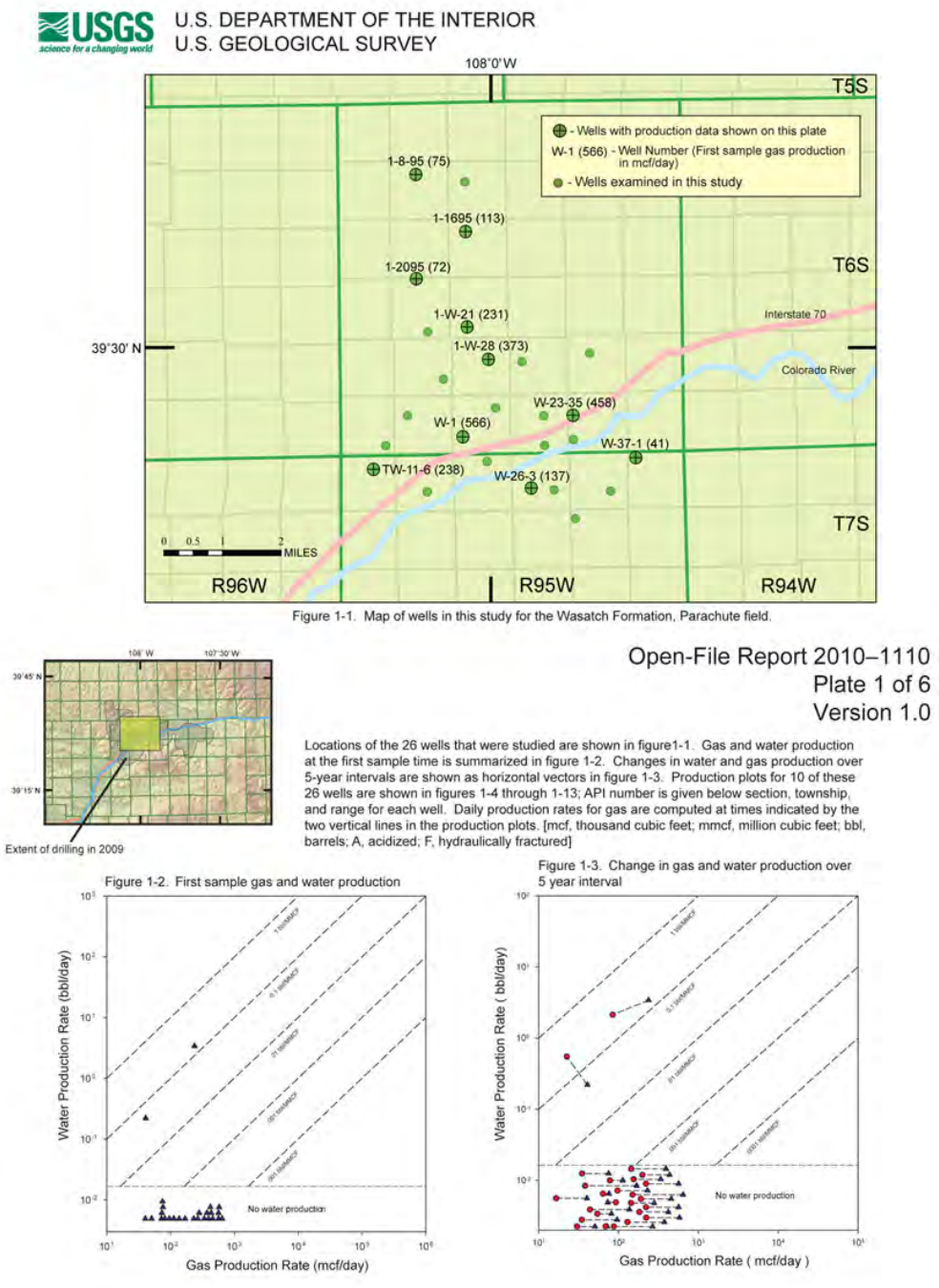

Figure 14. Gas and water production from the Wasatch Formation, Parachute Field, Piceance Basin, Colorado. Figure modified from Nelson and Santus (2010).

7. References Cited

Blackwell, D. D. and M. Richards, 2004. "Calibration of the AAPG geothermal survey of North America BHT data base." American Association of Petroleum Geologists Meeting, Dallas Texas, April 2004, Southern Methodist University Geothermal Lab Poster on BHT Calibration, *URL:* http://smu.edu/geothermal/BHT/BHT.htm, last accessed 2011-5-10.

Casillas, H. A., 2004, An Integrated Geophysical Study of the Uncompahgre Uplift, Colorado and Utah, M. S. Thesis,

Harrison, W. E., M. L. Prater, and P. K. Cheung, 1983. "Geothermal resource assessment in Oklahoma." Oklahoma Geological Survey, Norman, OK, *Special Publication 83-1*, 42 pp., 3 plates.

Morgan, P., 2009. "A preliminary analysis of geothermal resources in the central Raton Basin, Colorado, from bottom-hole temperature data." Geothermal Resources Council, *Transactions*, v. 33, p. 509-513.

Nelson, P. H., and S. L. Santus, 2010, "Gas, oil, and water production form Grand Valley, Parachute, Ruleson, and Mamm Creek Fields in the Piceance Basin, Colorado," U. S. Geological Survey Open File Report 2010-1110, Reston, VA, 28 pp., 6 plates, 3 tables, 6 digital appendices.

Quigley, M. D., 1965, Geologic history of Piceance Creek-Eagle Basins, *Bull. Am. Assoc. Petrol. Geol., 49*, 1974-1996.